ISSN 1392–1320 MATERIALS SCIENCE (MEDŽIAGOTYRA). Vol. XX, No. X. 2022

Dielectric and Electrical Properties of Copper-Polyimide-Copper Structures

Julia FEDOTOVA

Institute for Nuclear Problems of Belarusian State University, 220006 Minsk, Bobrujskaya str., 11, Belarus

crossref http://dx.doi.org/10.5755/j02.ms.28912

Received 16 April 2021; accepted 09 June 2021

Experimental study of current-voltage (*I-V*) characteristics and frequency dependences of impedance in copper-Kapton-copper structures in the temperature range 240 – 300 K were carried out. Concentration and mobility of charge carriers thermally excited from traps with exponential distribution by energy in Kapton bulk and metal-Kapton interface and injected from copper electrodes into Kapton were estimated from the fitting of experimental *I-V* curves within the frame of the model of the space charge limited current (SCLC). Concentration and the width of energy of localized states, arising from the disorder of the Kapton structure, are additionally estimated from the *I-V* characteristics.
Keywords: polyimides, Kapton, carrier transport mechanisms.

1. INTRODUCTION

Aromatic polyimides (PI) are very common among modern polymeric materials because they have a wide range of functional properties [1, 2]. On the one hand, due to significant polar bonds between molecular chains, PIs have high thermal stability, outstanding mechanical and electrical characteristics, which allow them to be widely used in several industrial products [2 – 14]. On the other hand, the high dielectric characteristics of thin PI films make it possible to use them as insulating layers in ultra-large integrated circuits. The latter is also due to the good ability of the PI films to planarize, low values of mechanical stresses, and high voltages of electrical breakdown. In addition, according to [14, 15], PI films have a lower dielectric constant ε (no higher than 3.5 – 4.0) compared, for example, with silicon oxide and silicon, due to the formation of pores during crosslinking of molecules of the PI structure. This makes PI films preferable (in comparison with silicon oxide) for achieving the maximum possible operation speed of electronic devices while decreasing their size [2].

In addition to the applications described, we can expect that PI films can serve as suitable substrates for the formation of various types of hybrid structures (HS), for example, in combination with metal, semiconductor, graphene, or other two-dimensional layers. In this case, interesting possibilities for electronics can be provided by PI films made in the form of porous membranes with artificially formed vertical channels (pores). For example, in hybrid structures of the PI/graphene, obtained by transferring CVD graphene layers onto a porous PI membrane, breaks in the graphene layer will be formed over the pores due to the internal stresses. The latter can lead to the "opening" of the forbidden zone in the graphene layer [16], which makes it possible to create field-effect transistors, various sensors, and other devices based on such HSs. To implement this idea, it is necessary to study the changes introduced by the graphene layer to the electronic transport in the metal/membrane/metal/graphene /metal HS. However, before studying this kind of HS, it is necessary to understand the changes in the carrier transport properties that are introduced into the PI substrate itself by the pores, as well as by deposited metallic layers (to form ohmic electrical contacts and/or Schottky barriers, etc.). These changes in the electron transport characteristics of substrate will be determined not only by the transformation of the structure of the PI layer itself (for example, due to the formation of pores) but also, to a large extent, by the properties of the pore surface and interfaces such as PI/metal.

Low values of dielectric constant and high resistivity of PI films, which make it possible to use them in electronics, are determined by the presence of dipoles, which often determine the mechanisms of charge carrier transport in them in both direct and alternating currents. The electrical and dielectric properties of PI films measured in AC/DC electric fields and described in the literature strongly depend on the structural features of the dipoles existing in them, which are determined by the method of film production. The AC/DC electrical properties for pure (undoped) PI films from different manufacturers, depending on their structure and external influences, were studied in a set of papers [9 – 15, 19 – 31]. They showed that above room temperatures and in electric fields up to 1 MV/m in undoped PI, five main mechanisms of carrier transport predominate – Richardson-Schottky, Poole-Frenkel, Fowler-Nordheim, Mott-Gurney (limited current space charge), as well as hopping of electrons and (or) ions under the influence of temperature and electric field. In some cases, in a wide range of temperatures (300 - 600 K), combinations of these mechanisms are possible, while the hopping contribution of ions is usually observed in strong electric fields and at the highest temperatures [19 – 23]. At the same time, it should be stated that due to the high resistivity of PI, the indicated mechanisms of charge carrier transport have not been studied below room temperature. However, high resistance (stability) of PI substrates to low temperatures impact, one can hope for their application in cryogenic power electronics and sensors designing.

* Corresponding author. Tel.: +375-29-6326075; fax: +375-17-253 11 24.
E-mail address: *julia@hep.by* (J. Fedotova)

Therefore, this work is focused on the detailed study of the mechanisms of charge carriers transport in the undoped PI films of the Kapton type (before the formation of pores and the hybrid structures with graphene themselves) based on the study of the temperature dependences of the current-voltage (*I-V*) characteristics and the frequency dependences of the impedance of copper-Kapton-copper structures.

2. EXPERIMENTAL

In this work, we investigated flat copper-Kapton-copper structures, on which DC *I-V* characteristics at different temperatures as well as frequency dependences of impedance at room temperature were measured when an electric field bias was applied normally to the plane of the polymer film. Copper layers with a thickness of $d = 80$ nm were sputtered on both sides of a 40 μm thick Kapton film. After fabrication of the copper-Kapton-copper structure, specimens with dimensions of 2×3 mm^2 were cut from it.

To measure the electrical properties, thin copper wires were attached by silver paste to the copper contact layers of the structure. Then we soldered wires to the gold-plated electrical contacts of a special measuring cell. The cell with the soldered sample was connected to the cryogenic plug of the measuring probe, the upper part of which was connected to the measuring systems using a special connector. In the study of the *I-V* characteristics, we used a Keithley 6430 power supply-current meter and a Keithley 3485 voltmeter [17].

Agilent-type LCR meters were used to measure the impedance in the frequency range 20 Hz – 2 MHz. To measure *I-V* characteristics, the lower part of the probe with the sample to be measured was placed in a CFHF cryogenic system (Cryogenics Ltd., England) based on a closed-cycle refrigerator. The CFHF setup made it possible to measure the *I-V* characteristic at direct current and the frequency dependences of the impedance with an accuracy of 0.1 % in the temperature range $100 < T < 310$ K in an automated mode. When *I-V* measuring, the sweep of the bias voltage *V* was carried out at a rate of 0.1 V/s.

A diagram of the test station for measuring the electrical properties of samples was explained in [18] in detail. To record the parameters of two samples simultaneously, the test station included two HIOKI 3532 LCR HiTESTER impedance meters with frequencies in the range of 50 Hz to 5 MHz.

To measure and control temperature the Lakeshore 340 controller was used, which made it possible to stabilize the temperature with an accuracy of 0.005 K during the sweep of the bias voltage or the frequency of the alternating field applied. The temperature of the samples was measured by LakeShore thermal diodes, which were calibrated with an accuracy of 0.0005 K and had a reproducibility of 0.001 K. Due to the high resistance of the Kapton layer (which exceeded 100 – 120 MΩ at room temperature) and the limited input resistance of the Keithley 3485 voltmeter (not above 20 GΩ), the *I-V* characteristics and impedance could be measured with an accuracy of about 10 % only at temperatures above 150 – 200 K. At lower temperatures, the resistance of the samples reached values of more than 1 GΩ and the results could not be considered reliable.

3. RESULTS

A comparison of the frequency dependences of the phase angle $\theta(f)$ and the specific total impedance $Z(f)$ for copper-Kapton-copper samples is shown in Fig. 1. As can be seen, the θ-values are negative, that confirms the capacitive type of the equivalent circuit of the studied structures (see inset in Fig. 1 b). The capacitive behavior of the studied structures is also evidenced by the decrease in impedance when frequency increasing in Fig. 1 b. In addition, it follows from the figure that the shape of the $Z(f)$ curves fully corresponds to the heterogeneity of the structure of samples. The $Z(f)$ below 500 Hz reflects the frequency independence of the impedance of metal contacts. Linearization of the $Z(f)$ curves in double logarithmic coordinates at frequencies above 5 kHz indicates that an AC hopping conduction mechanism is possible in Kapton films in the form of the well-known Mott's law $Z(f) \sim f^{-k}$ [25 – 27], realized in disordered systems on the dielectric side of the metal-insulator transition. The experimentally obtained value of the exponent $k \approx 0.96$ turned out to be somewhat different from the classical value 0.8 for the Mott mechanism for disordered semiconductors. The power-law character of $Z(f)$ was observed earlier in [19 – 21] not only in PI films, including Kapton, but also in other polymers. The capacitive behavior of the studied structures and presence of hopping contribution to the electron transport in them indicates that the main contribution to the RC element in the equivalent circuit in the inset to Fig. 1 b is introduced precisely by the polymer film, although a certain role of the metal-insulator interface is not excluded.

The capacitor-like behaviour of the impedance of the copper-Kapton-copper structure under study allows one to extract, from impedance measurements, the frequency behaviour of the Kapton film capacitance, which, as it turned out, follows the relationship $C = 1/(2\pi \cdot f \cdot Z)$ without noticeable error. The indicated dependences $C(f)$ shown in the inset to Fig. 1 b, made it possible to estimate the dielectric constant of the Kapton using the relation $\varepsilon = C_d/(\varepsilon_0 \cdot S)$, where d is the thickness of the polymer film, S is the area of the capacitor (structure), and ε_o is the dielectric constant of vacuum. The evaluation showed that in the studied samples of the Kapton film the value $\varepsilon \approx 3.7$, which is very close to the values given in the reference work of the DuPont company [1] and other studies [2 – 15].

We also should note that a rapid increase in capacitance (and, consequently, dielectric constant) with decreasing frequency (especially below 500 kHz) may indicate sufficiently high mobility of charge carriers in a Kapton film. The latter means that at room temperature mobile carriers can drift over sufficiently large distances, despite the disorder of their structure, as a result of which the current paths in Kapton form a continuous percolation network. The monotonic behaviour of the $C(f)$ curves (the absence of peaks) indicates that, at least at room temperature, the studied films lack all kinds of dipole relaxation.

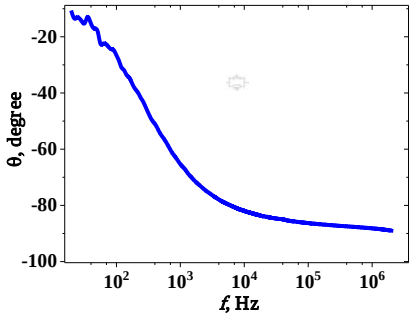

a

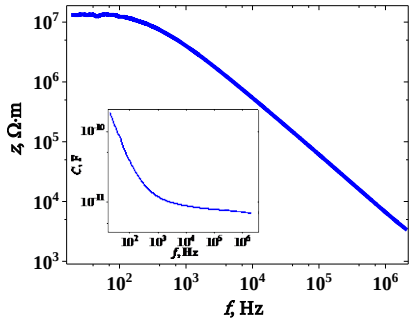

b

Fig. 1. a – dependences of the phase shift angle θ; b – specific impedance Z on frequency for copper-Kapton-copper structure. a inset shows the equivalent circuit of the structure (C_c is the Kapton capacity, RC is the electrical resistance of the structure). b inset shows the dependence of capacitance on frequency for copper-Kapton-copper structure

The experimental transversal I-V characteristics $j(E)$ in the copper-Kapton-copper structures measured (j is the current density, E – the bias electric field intensity) are shown in Fig. 2. To reveal the mechanisms of charge carrier transport in the studied structure at low temperatures, the $j(E)$ curves were rearranged in different scales that corresponded to different models for the description of I-V characteristics. Quite often in the literature, to describe the I-V characteristics of polyimides, the well-known relation

$$j = AT^2 \exp\left(-\frac{\varphi_b - \beta E^{1/2}}{kT}\right), \quad (1)$$

is used, which describes either trap-enhanced tunnelling through a polymer layer (Poole-Frenkel mechanism) or emission of charge carriers from a metallic electrode into a polymer (Schottky-Richardson mechanism) [15, 16, 23, 26, 7, 30, 31].

Re-plotting the I-V characteristics in the coordinates $\mathrm{Ln}\,(j/\mathrm{AT}^2) - E^{1/2}$ for these models makes it possible to estimate the values of the barrier height φ_b, overcome by charge carriers injected from the metal contact into the polymer layer, and the coefficient β, the value of which makes it possible to determine which of the two mechanisms most adequately describes $j(E)$ curves. In accordance with the model, I-V curves in such coordinates should be linearized in the region of weak fields (i.e., at the initial portions of the I-V characteristics), however, in our case, the linearization was achieved on the contrary in the region of strong bias fields $E > (1-100)\cdot 10^4$ V/m, where above room temperature the Fowler-Nordheim model is considered valid [15, 16, 23, 26, 27, 30, 31]. This fact, as well as the physically unreal values of the coefficient β (<< 1), obtained from the linearization of this type, meaning that mechanisms of type (1) are not suitable for describing low-temperature I-V characteristics in the studied Cu-Kapton-Cu structures.

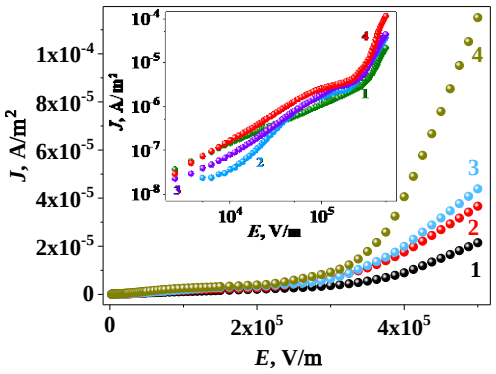

Fig. 2. I-V characteristics of copper-Kapton-copper structure on a linear scale at temperatures of: 1 – 240 K; 2 – 260 K; 3 – 280 K; 4 – 300 K. Inset: example of I-V characteristics of the copper-Kapton-copper sample at 300 K in log-scale

Rebuilding the I-V characteristic in the coordinates $\mathrm{Ln}(j/E^2) - E^{-1}$ for the Fowler-Nordheim model

$$j(E,T) = 1{,}54\cdot 10^{-6}\cdot\frac{E^2}{\varphi_b}\exp\left(-6{,}7\cdot 10^6\frac{\varphi_b^{\frac{3}{2}}}{E}\right), \quad (2)$$

gave linearization in weak rather than strong electric fields with unphysically low values of the barrier height (below 10^{-9} eV), which indicates the unfairness of this model too for the studied structures.

The impossibility to use models Eq. 1 and Eq. 2 for the description of low-temperature I-V characteristics in the studied structures is quite understandable, since, according to the literature data, these mechanisms manifest themselves only at much higher than room temperature [15, 21 – 23].

Mott and Gurney [27, 32] proposed the injection model to describe the I-V characteristics in metal-dielectric-metal structures

$$j(E,T) = en(T)\cdot\mu(T)\cdot E + \varepsilon\varepsilon_o\mu(T)\cdot\frac{E^2}{d}, \quad (3)$$

where d is the thickness of dielectric; n and μ are the concentration and mobility of the thermally excited free equilibrium charge carriers. This model, called the ideal Mott-Gurney model, was based on the mechanism of space charge limited current (SCLC). As follows from the first term in relation Eq. 3, the initial (low bias field) part of I-V characteristics is described by Ohm's law [26, 27, 32]. According to [15, 16, 27, 32, 33], in higher fields, there is a transition from linear to square-like I-V characteristic law – the second contribution to relation Eq. 3. This contribution is realized when the concentration of charge

carriers injected from the metallic electrode under the electric field impact begins to exceed the concentration of equilibrium free charge carriers generated by thermal vibrations of the lattice.

As seen from Fig. 3, re-plotting of *I-V* curves in double logarithmic scale (in the framework of the ideal Mott-Gurney model) indeed gives two linear sections with different slopes. In the region of low bias fields ($E < 2 \cdot 10^4$), this slope varied from 0.87 at $T = 240$ K to 1.27 at $T = 300$ K, lower is close to 1, in accordance with the first contribution to the model (3). However, at the highest electric fields ($E > 3 \cdot 10^5$), the slope of the straight line (exponent at E) turned out to be significantly higher than two, reaching values of the order of 3-4 (see Table 1), which does not correspond to relation Eq. 3 for the ideal SCLC model.

In this regard, for fitting of *I-V* curves based on Eq. 3, its high-field contribution was replaced by the combined Mark-Helfrich relation [26, 32]:

$$J(E) = en(T) \cdot \mu(T) \cdot E + e\mu N_C \left[\frac{\varepsilon \varepsilon_o m}{eN_t(m+1)} \right] \left[\frac{2m+1}{m+1} \right] \frac{E^m}{d^{2m}}, \quad (4)$$

where N_C is the effective density of delocalized states in the allowed band; N_t is the concentration of traps in the "tail" of localized states in the allowed band, respectively, and the exponent $m = E_{ch}/kT$ depends on the energy width E_{ch} of "tail" localized states with exponential energy distribution of traps, occupied by carriers. Eq. 4 is called the advanced SCLC model.

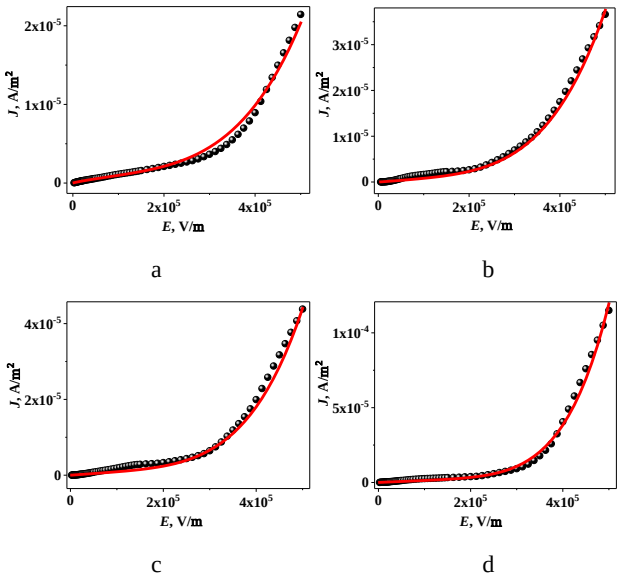

Fig. 3. Experimental (dots) and fitted (solid lines) dependences of the current density on the electric field intensity for copper-Kapton-copper structure in linear scale for temperatures T: a – 240 K; b – 260 K; c – 280 K; d – 300 K

As seen from Fig. 3, the fitting of *I-V* curves based on the combined model of Mott-Gurney and Mark-Helfrick Eq. 4 results, in a whole, to the satisfactory reflecting of experimental j(E) curves behaviour both in the low-field region (linear contribution) and in strong fields (power contribution). Estimates of the model parameters for these regions of the electric field, given in Table 1, gave acceptable and physically justified values both for the concentration and energy bandwidth of localized "tail" states (traps), and for the mobility and concentration of free charge carriers in Kapton.

Table 1. Fitting parameters of $J(E, T)$ dependences for the combined Mott-Gurney and Mark-Helfrick model

T, K	m (E > 10^5 V/m)	E_{ch}, eV	N_t, m^{-3}	μ, m^2/V·s	n, m^{-3}
240	2.99	$8.30 \cdot 10^{-2}$	$3.75 \cdot 10^{19}$	$2.2 \cdot 10^{-7}$	$3.05 \cdot 10^{14}$
260	3.20	$9.41 \cdot 10^{-2}$	$3.01 \cdot 10^{19}$	$2.1 \cdot 10^{-7}$	$1.09 \cdot 10^{14}$
280	3.50	$1.09 \cdot 10^{-1}$	$1.92 \cdot 10^{19}$	$8.0 \cdot 10^{-8}$	$6.17 \cdot 10^{14}$
300	4.50	$1.42 \cdot 10^{-1}$	$1.09 \cdot 10^{19}$	$1.1 \cdot 10^{-7}$	$6.85 \cdot 10^{14}$

And although there are no data on these values in the literature on Kapton for low temperatures, the values obtained at room temperature agree quite satisfactorily with the literature data [32 – 34]. In conclusion, it should be noted that the observed deviations of simulated curves $j(E)$ from the experimental ones in the region of intermediate values of the bias electric field (see Fig. 3 b, c, d) in polymers are usually attributed to the transition of the *I-V* characteristics to the regime of the limiting filling of traps in this range of fields with increasing temperature [34].

4. CONCLUSIONS

Experimental study and modelling of the *I-V* characteristics in copper-Kapton-copper structures in the temperature range 240 – 300 K were carried out, and their impedance was measured at room temperature. It is shown that the dielectric constant of the studied Kapton layer was 3.77, which well coincides with the known literature data. Experiments have shown that the *I-V* characteristics of such structures are satisfactorily described on the basis of the model of the space charge limited current (SCLC). The application of the SCLC model allows to estimate the concentration and mobility of charge carriers, which are (i) thermally excited from traps with exponential distribution by energy in Kapton bulk and metal-Kapton interface and (ii) injected from copper electrodes into Kapton in the temperature range of 240 – 300 K. In addition, the concentration and the width of energy of localized states, arising due to the disorder of the Kapton structure, was estimated from the *I-V* curves.

Acknowledgments

The author would like to acknowledge the financial support from the State Scientific Research Programme "Photonics and electronics for innovations", project 3.2.5.

REFERENCES

1. Dupont Kapton. Summary of properties. Bulletin "Kapton® Polyimide Film – Products of Decomposition" (H-16512): https://www.dupont.com/content/dam/dupont/amer/us/en/products/ei-transformation/documents/EI-10142-Kapton-Summary-of-Properties.pdf
2. **Ghosh, M. K., Mittal, K.L.** Polyimides: Fundamentals and Application, Plastics engineering (Marcel Dekker, Inc.), 36; New York, 1996: p. 891.

3. **Liang, T., Makita, Y., Kimura, S.** Effect of Film Thickness on The Electrical Properties of Polyimide Thin Films *Polymer* 42 2001: pp. 4867 – 4882. https://doi.org/10.1016/S0032-3861(00)00881-8
4. Advanced Polyimide Materials: 1st Edition. Synthesis, Characterization and Applications, Editor Shi-Yong Yang. Elsevier, eBook ISBN 9780128126417. 2018: pp. 498.
5. **Chern, Y.T., Shiue, H.C.** Low Dielectric-Constants of Soluble Polyimides Based on Adamantane *Macromolecules* 30 (16) 1997: pp. 4646 – 4651. https://doi.org/10.1021/ma970520n
6. **Bei, R., Qian, Ch., Zhang, Y., Chi, Zh., Liu, S., Chen, X., Xu, J., Aldred, M.P.** Intrinsic Low Dielectric Constant Polyimides: Relationship Between Molecular Structure and Dielectric Properties *Journal Materials Chemistry C* 5 2017: pp. 12807 – 12815. https://doi.org/10.1039/ C7TC04220E
7. **Diaham, S., Locatelli, M.L., Lebey, T.** Improvement of Polyimide Electrical Properties During Short-Term of Thermal Aging *Annual Report Conference on Electrical Insulation Dielectric Phenomena* 2008: pp. 79 – 82. https://doi.org/10.1109/CEIDP.2008.4772840
8. **Ha, C.S., Mathews, A.S.** Polyimides and High-Performance Organic Polymers *Advanced Functional Materials* 2021: pp. 1 – 36. https://doi.org/10.1007/978-3-642-19077-3_1
9. **Loke, A.L.S.** Process Integration Issues of Low-permittivity Dielectrics with Copper for High-performance Interconnects. Ph.D. Thesis, Stanford University, 1999. https://doi.org/10.13140/RG.2.1.2425.5766
10. **Wang, J., Jin, K., He, F., Sun, J., Fang, Q.** A New Polymer with Low Dielectric Constant Based on Trifluoromethyl Substituted Arene: Preparation and Properties *RSC Advances* 4 2014: pp. 40782 – 40787. https://doi.org/10.1039/x0xx00000x
11. **Lee, Ch., Shul, Y., Han, H.** Dielectric Properties of Oxydianiline-Based Polyimide Thin Films According to the Water Uptake *Journal of Polymer Science B*: *Polymer Physics* 40 2002: pp. 2190 – 2198. https://doi.org/10.1002/polb.10277
12. **Chisca, S., Sava, I., Musteata, V.E., Bruma, M.** Dielectric and Conduction Properties of Polyimide Films *Annual Report Conference on Electrical Insulation Dielectric Phenomena* 2011. pp. 253 – 256. https://doi.org/10.1109/SMICND.2011.6095784
13. **Deligoez, H., Yalcinyuva, T., Ozguemus, S., Yildirim, S.** Electrical Properties of Conventional Polyimide Films *Journal of Applied Polymer Science* 100 2006: pp. 810 – 818. https://doi.org/10.1016/j.polymer.2005.02.097
14. **Muruganand, S., Narayandass, S.K., Mangalaraj, D., Vijayan, T.M.** Dielectric and Conduction Properties of Pure Polyimide Films *Polymer International* 50 2001: pp. 1080 – 1084. https://doi.org/10.1002/pi.749
15. **Blythe, A.R.** Electrical Properties of Polymers. Cambridge University Press, New York, 1979: pp. 1 – 475.
16. **Xu, P., Yang, J., Wang, K., Zhou, Z., Shen, P.** Porous Graphene: Properties, Preparation, and Potential Applications *Chinese Science Bulletin* 57 (23) 2012: pp. 2948 – 2955. https://doi.org/10.1007/s11434-012-5121-3
17. **Fedotov, A.K., Prischepa, S.L., Fedotova, J.A., Bayev, V.G., Ronassi, A.A., Komissarov, I.V., Kovalchuk, N.G., Vorobyova, S.A., Ivashkevich**, **O.A.** Electrical Conductivity and Magnetoresistance in Twisted Graphene Electro-Chemically Decorated with Co Particles *Physica E: Low-dimensional Systems and Nanostructures* 117 2019: pp. 1 – 11. https://doi.org/10.1016/j.physe.2019.113790
18. **Koltunowicz, T.** Measurement Station for Frequency Dielectric Spectroscopy of Nanocomposites and Semiconductors *Journal of Applied Spectroscopy* 82 2015: pp. 653 – 658. https://doi.org/10.1007/s10812-015-0158-0
19. **Bellucci, F., Khamis, I., Senturia, S.D., Latanision, R.M.** Moisture Effects on the Electrical Conductivity of Kapton Polyimide *Journal of the Electrochemical Society* 137 2006: pp. 1778 – 1784. https://doi.org/10.1149/1.2086797
20. **Kim, T.Y., Kim, W.J., Lee, T.H., Kim, J.E., Suh, K.S.** Electrical Conduction of Polyimide Films Prepared from Polyamic Acid (PAA) and Preimidized Polyimide (PI) Solution *eXPRESS Polymer Letters* 1 (7) 2007: pp. 427 – 432. https://doi.org/10.3144/expresspolymlett.2007.60
21. **Nevin, J.H., Summe, G.L.** DC conduction mechanisms in thin polyimide films *Microelectronics Reliability* 21 (5) 1981: pp. 699 – 705. https://doi.org/10.1016/0026-2714(81) 90061-5
22. **Ansari, A.A., Al-Marzouki, F.M.** Electrical Conduction in Polyimide Films *Indian Journal of Physics A* 73 (6) 1999: pp. 789 – 792. https://core.ac.uk/download/pdf/158963398.
23. **Sessler, G.M., Hahn, B., Yoon, D.Y.** Electrical Conduction of Polyimide Films *Journal of Applied Physics* 60 (1) 1986: pp. 318 – 326. https://doi.org/10.1063/1.337646
24. **Lamb, D.R.** Electrical Conduction Mechanisms in Thin Insulating Films, London, Methuen, 1967: pp. 130.
25. **May, P.W., Hohn, S., Wang, W.N., Fox, N.A.** Field Emission Conduction Mechanisms in Chemical Vapour Deposited Diamond and Diamond-Like Carbon Films *Applied Physics Letters* 72 (17) 1998: pp. 2181 – 2184. https://doi.org/10.1016/S0925-9635(99)00074-6
26. **Mark, P., Helfrich, W.** Space-Charge-Limited Currents in Organic Crystals *Journal of Applied Physics* 33 (1) 1962: pp. 205 – 215. http://dx.doi.org/10.1063/1.1728487
27. **Mott, N.F., Gurney, R.W.** Electronic Processes in Ionic Crystals, Clarendon Press, Oxford, 1940: pp. 1 – 293. https://doi.org/10.1021/j150412a015
28. **Mott, N.F., Davis, E.A.** Electronic Processes in Non-crystalline Materials, 2nd ed. Oxford, *Contemporary Physics.* 55 (4) 1979: pp. 1 – 337.
29. **Böttger, H., Bryksin, V.V., Schulz, F.** Hopping Transport in the Three-site Model in the Presence of Electric and Magnetic Fields: Rate Equation and Transport Phenomena for Small Polarons *Physical Review B* 48 (1) 1993: pp. 161. https://doi.org/10.1103/PhysRevB.48.161
30. **Sze, S. M.** Physics of Semiconductor Devices, New York: Wiley, 3rd ed., 2006.
31. **Lampert M. A., Schilling, R.B.** Chapter 1 Current Injection in Solids: The Regional Approximation Method *Semiconductors and Semimetals* 6 1970: pp. 1 – 96. https://doi.org/10.1016/S0080-8784(08)62630-7

32. **Rohr, J.A.** Measurements and Modelling of Space-Charge-Limited Current Transport in Organic Single-Carrier Devices. PhD thesis, Imperial College London, 2018. Rohr-J-2018-PhD-Theses.pdf

33. **Rose, A.** Space-Charge-Limited Currents in Solids *Physical Review* 97(6) 1955: pp. 1538 – 1544. https://doi.org/10.1103/PhysRev.97.1538

34. **Il'yasov, V.Kh., Lachinov, A.N., Moshelev, A.V., Ponomarev, A.F.** Estimation of the Parameters of Charge Carriers in Polymers in the Vicinity of the Threshold of Thermally Stimulated Switching *Physics of Solid State* 50 (3) 2008: pp. 568 – 572. https://doi.org/10.1134/ S1063783408030293